JOURNAL OF CATALYSIS 143, 325–344 (1993)

Reactivity of Molybdovanadophosphoric Acids: Influence of the Presence of Vanadium in the Primary and Secondary Structure

DANIELE CASARINI,* GABRIELE CENTI,†,[1] PAVEL JÍRŮ,‡ VIRGINIA LENA,† AND ZDENA TVARŮŽKOVÁ

*Dipartimento di Chimica Organica and †Dipartimento di Chimica Industriale e dei Materiali, Università di Bologna, Viale del Risorgimento 4, 40136 Bologna, Italy; and ‡J. Heyrovský Institute of Physical Chemistry and Electrochemistry, Academy of Sciences of the Czech Republic, Dolejškova 3, 182-23 Prague 8, Czech Republic

Received June 8, 1992; revised February 18, 1993

The catalytic behavior in butadiene and *n*-butane oxidation of molybdovanadophosphoric acids with vanadium localized inside the primary (oxoanion) and/or the secondary structure is reported. The samples are characterized by infrared, ^{31}P-NMR, ^{51}V-NMR, and UV–visible diffuse reflectance spectroscopies in order to obtain information on the nature and localization of vanadium in the samples before reaction and the possible changes occurring during the course of the catalytic reaction. In particular, it is shown that vanadium localized initially in the secondary structure can exchange with the molybdenum atoms of the oxoanion during the catalytic reaction. Introduction of vanadium in the molybdophosphoric acid structure enhances the selective formation of maleic anhydride from butadiene when vanadium is present both inside the oxoanion or localized in the secondary structure (before the catalytic tests), but the maximum in catalytic performance is found for different amounts of vanadium, depending on where the vanadium is localized initially. However, when present in the secondary structure, vanadium also has a negative influence on the activity of the heteropoly acid. On the contrary, in *n*-butane oxidation, the presence of vanadium enhances the rate of alkane activation due to the different rate-determining step. The presence of V ions also affects the maximum selectivity and yield to maleic anhydride from butane. V ions in the secondary structure are more selective at low conversion, while V ions inside the oxoanion are more selective at higher conversions and thus allow better maximum yields to maleic anhydride.

INTRODUCTION

For several years heteropoly compounds of the Keggin type (*1*) have attracted scientific interest as solid catalysts due to their acid–base and redox catalytic properties (*2, 3*). These compounds can be considered as molecular solids. Their structure consists of the heteropoly anion molecules (*primary* structure) linked in a three-dimensional arrangement by the counter-cations and the water molecules of coordination (*secondary* structure). Various elements can be substituted for the components of the heteropoly anion or the counter-cations in order to modify their catalytic properties (*2, 3*). Heteropoly acids containing both Mo and V, in particular, show interesting catalytic properties in both heterogeneous and homogeneous phases. In the heterogeneous case, with gas-phase reactants, molybdovanadophosphoric acid based catalysts are used commercially for the synthesis of methacrolein and isobutyric acid to methacrylic acid (*2*) due to their enhanced redox properties. Interesting results have been obtained with various other reactions of selective oxidation, such as methanol and acrolein oxidation to formaldehyde and acrylic acid, respectively (*4*), and recently also in the selective oxidation of alkanes (*n*-butane and *n*-pentane) (*5–7*).

Usually, in all these catalysts vanadium is introduced in the oxoanion by substitution

[1] To whom correspondence should be addressed.

0021-9517/93 $5.00

of one or more molybdenum atoms. The redox, acid–base and thermal stability properties of these vanadophosphomolybdo–heteropoly compounds are influenced considerably by the degree of substitution (*2–11*). However, there is no clear documentation in the literature regarding the problem of whether or not the simple addition of a vanadium component to the $H_3PMo_{12}O_{40}$ acid leads to very different catalytic performances in selective oxidation reactions as compared with the corresponding heteropoly acids with vanadium localized in the primary structure. The only available data are those of Kutyrev *et al.* (*10*), who report different catalytic functions for transition metals in cationic or anionic positions and the necessity of having pair centers for selective behavior, especially in butane oxidation.

The objective of the research reported in this paper was therefore to compare the catalytic behavior of vanadophosphomolybdic acids containing vanadium in the oxoanion with that of samples prepared by adding a vanadium salt to $H_3PMo_{12}O_{40}$ acid. In the latter case vanadium is assumed to be in the secondary structure. The selective oxidation of *n*-butane and of butadiene were chosen as model reactions for this study. In fact, butadiene is an intermediate in *n*-butane selective oxidation to maleic anhydride and thus the comparison of these reactions makes it possible to analyze the role of the localization of vanadium in the steps of hydrocarbon activation by oxidative dehydrogenation (rate-determining step in alkane oxidation) and on the step of oxygen insertion (rate-determining step in butadiene oxidation).

EXPERIMENTAL

Preparation of the samples. The pure heteropoly acids ($H_{3+n}PV_nMo_{12-n}O_{40} \cdot xH_2O$), where n = 0–2, were prepared using the method of Tsigdinos and Hallada (*12*). An aqueous solution (100 cm^3) containing Na_2HPO_4 (7.1 g) was added to a hot aqueous solution (100 cm^3) containing sodium metavanadate in such an amount as to have the appropriate P : V ratio (for example, 12.2 g for the preparation of $H_5PV_2Mo_{10}O_{40}$). After the mixture had cooled to room temperature, 5 cm^3 of concentrated H_2SO_4 were added slowly, drop by drop. Then, after it was cooled to room temperature, the heteropoly acid was extracted in ether as liquid heteropoly etherate. The molybdovanadophosphoric acid crystallized from this solution (by drying in a flow of air) was recrystallized in water. The resulting solid was first dried at 70°C, then at 120°C overnight, and finally calcined at 350°C (air, 3h).

The heteropoly acids obtained using this method were used as such for the catalytic tests or for the preparation of the compounds with vanadium in the secondary structure using the following method. An aqueous solution containing VO^{2+} ions in the appropriate amount was prepared by reaction of V_2O_5 with oxalic acid at about 100°C. After complete dissolution of the V oxide, the solution was cooled to room temperature and the $H_{3+n}PV_nMo_{12-n}O_{40}$ compound which was previously calcined and stored in a water-free atmosphere (in order to avoid readsorption of water of crystallization) was added. The water was then removed from the solution by evaporation, and the resulting solid dried and calcined as in the case of pure heteropoly acid compounds.

The surface area of these samples, determined by the BET method (N_2 adsorption), is always low, 4–8 m^2/g, and there is no significant difference between the sample containing vanadium in the oxoanion and those prepared by addition of the vanadium salt to $H_3PMo_{12}O_{40}$ or $H_5PMo_{10}V_2O_{40}$ acids.

The following symbols are used hereafter to refer to these compounds:

V0, V1, V2: $H_{3+n}PV_nMo_{12-n}O_{40}$ with n = 0–2, respectively;

V0 + nV (n = 1, 2): $H_3PMo_{12}O_{40}$ compound salified with VO^{2+} with a $VO^{2+}/H_3PMo_{12}O_{40}$ molar ratio equal to n;

V2 + nV (n = 1, 2): $H_5PV_2Mo_{10}O_{40}$ compound salified with VO^{2+} with a $VO^{2+}/H_5PV_2Mo_{10}O_{40}$ molar ratio equal to n.

The suffix "ar" indicates samples after the catalytic tests in butadiene oxidation.

Characterization of the samples. Catalytic tests were carried out using a fixed-bed flow reactor at atmospheric pressure. Three grams of catalyst with particle dimensions in the 0.250–0.590 mm range were used for the catalytic tests in order to avoid intraparticle diffusion limitations on the reaction rate. The reactant flow composition was 2.2% butane and 18% O_2 in helium, and the total flow rate was 1.8 liter/h. The catalytic measurements were made after the heteropoly compounds had been conditioned by flowing the reacting mixture for 2 h at the highest temperature of reaction at which the tests were carried out. The reactants and reaction products were analyzed using two on-line gas chromatographs, the first for organic products and the second for oxygen, nitrogen, and carbon oxides. The first operated with a flame ionization detector and a Porapak QS column. The second gas chromatograph was operated with a thermal conductivity detector and a Carbosieve-II column.

Infrared (IR) spectra were recorded with a Fourier-transform Perkin–Elmer 1750 instrument. Spectra in the skeletal vibration region (400–1200 cm^{-1}) were recorded using the KBr disc technique and calibrated amounts (0.1%) of heteropoly compound. Spectra for the characterization of the surface acidity were recorded using the self-supporting disc technique and conventional evacuation and gas manipulation lines. The pretreatment of the samples was evacuation at 180°C up to complete removal of crystallization and coordination water, as indicated by the disappearance of related IR bands and the change in the overtones of the ν(PO) and ν(MO) skeletal vibrations at around 2000 cm^{-1} (*6*).

^{31}P-NMR spectra were recorded at room temperature on a Bruker HFX-90 instrument spectrometer operating at 36.43 MHz using a deuterium lock. Samples were dissolved (0.2 *M* solution) in D_2O in 10-mm tubes. Peaks are relative to 85% H_3PO_4 as the external standard. Chemical shifts to low frequency of the reference are negative.

^{51}V-MAS-NMR spectra were recorded at room temperature on a Bruker CXP300 instrument equipped with a MAS rotor. Vanadium oxytrichloride ($VOCl_3$) in a sealed tube provided the external reference. The spinning rate was in the 3–5 kHz range (usually 4.2 kHz) and typically 20,000 transients were collected. ^{51}V-NMR spectra in solution were recorded on the same instrument.

UV–visible diffuse reflectance spectra were recorded on a Kontron UVICON 860 instrument with barium sulphate as the reference sample. The spectra were recorded in air at room temperature.

RESULTS

Characterization of the Samples

Infrared characterization. Reported in Fig. 1 is the infrared spectrum of the V1 compound and in the insets of the Figure, the bands at 1063 and 962 cm^{-1} are expanded and compared with those for the V0, V2, and V0 + 2V compounds. The characteristic bands of V0 ($H_3PMo_{12}O_{40}$) (*13*) are not modified by the addition of the vanadium component (V0 + 2V), suggesting that vanadium is not introduced in the oxoanion molecule. Instead, when the same number of vanadium atoms are present in the oxoanion (V2), a clear shift in the position of the bands is observed (Fig. 1 and Table 1). The shift is proportional to the number of vanadium atoms in the oxoanion (Table 1). In addition, when vanadium atoms are present in the oxoanion, a shoulder at about 1085 cm^{-1} is observed due to the lowering of the oxoanion symmetry, which, in addition to the shift in the position of the bands (Table 1), can be used to monitor the substitution of vanadium in the oxoanion. For all samples containing vanadium in the primary or secondary structure a shoulder is observed at about 990 cm^{-1}, the position of which is shifted about 30 cm^{-1} with respect to the $\nu_{V=O}$ band in crystalline V_2O_5 (1022 cm^{-1}). The absence of the band at 1022 cm^{-1} in V0 + nV and V2 + nV samples excludes

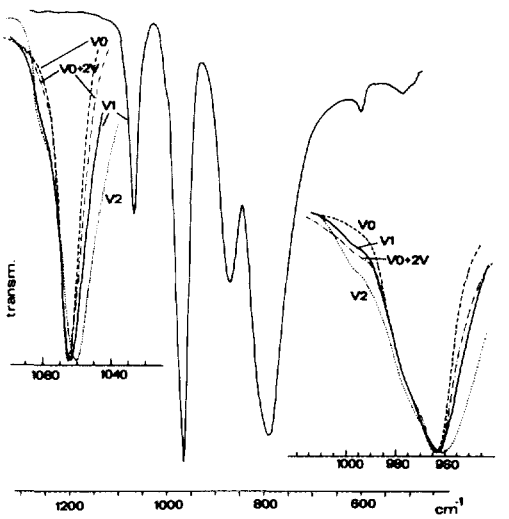

FIG. 1. FT-IR spectrum (KBr technique) of the V1 compound. In the inset, the bands at 1063 and 962 cm^{-1} are expanded and compared with those relative to V0, V2, and V0 + 2V compounds.

the possibility that the added V compound is present in these samples after calcination in the form of V_2O_5. In fact, additional tests with mechanical mixtures of H_3PO_4 and V_2O_5 in a molar amount equivalent to that of the VO + nV samples have shown that, when present, V_2O_5 is clearly detectable by IR characterization.

^{51}V-NMR data. The ^{51}V-MAS-NMR spectra of selected vanadophosphomolybdic samples before and after the catalytic tests are shown in Fig. 2. The spectra of the corresponding compounds in aqueous solution are reported in Fig. 3. Spectra of vanadium both in the solid state and in solution were recorded because even at a spinning rate of about 5 kHz, the ^{51}V-MAS-NMR spectra are dominated by the sideband pattern. The central transitions agree with those determined in solution, but in the latter case the narrow linewidth and the isotropic chemical shift allows a better differentiation between the V coordination environments. On the other hand, since the ^{51}V isotope (spin 7/2) has a nuclear electric quadrupole moment, the sideband pattern in the ^{51}V-MAS-NMR spectrum depends on the chemical shift anisotropy (*14, 15*) and thus can give useful information on the coordination environment. In addition, the MAS spectrum can indicate possible changes in the nature of the vanadium species which occur when the heteropoly compound is dissolved in water.

The ^{51}V-NMR spectrum in solution of the V1 compound (Fig. 3, spectrum 1) shows a single sharp peak centred at −531 ppm according to literature data (*16*) and that indicates the presence of only the $[PVMo_{11}O_{40}]^{4-}$ oxoanion. In the solid state, the ^{51}V-MAS-NMR spectrum (Fig. 2) shows a main envelope of side bands centred at around −300 ppm and a second poorly resolved envelope centred at around −700 ppm according to an axially symmetric shielding tensor (*14, 17*). Tests changing the spinning rate in the 3–5 kHz range show that the MAS center band corresponds to that indicated by the liquid experiments and suggests that the sideband pattern is determined by a single V species, in agreement with the liquid-phase ^{51}V-NMR data (Fig. 3).

When vanadium is added to H_3PO_4 (V0 + 1V), only a weak and not well resolved ^{51}V-MAS-NMR signal is observed centred at around −580 ppm (Fig. 2). The spectrum in solution (Fig. 3, spectrum 2) is characterized by a sharp signal at −532 ppm

TABLE 1

Shift in the Stretching Frequency of the Infrared Bands of $H_{3+n}PV_nMo_{12-n}O_{40}$ (n = 0–3) Heteropoly Acids as a Function of the Number of V Atoms in the Oxoanion

Compound	Stretching frequency (cm^{-1})			
	P–O_i	Mo–O_b	Mo–O_t	Mo–O_b
V0	1065	871	964	792
V1	1063	868	962	785
V2	1060	865	960	784
V3	1059	863	959	781

Note. O_i, O_t and O_b indicate inner, terminal, and bridging oxygen, respectively.

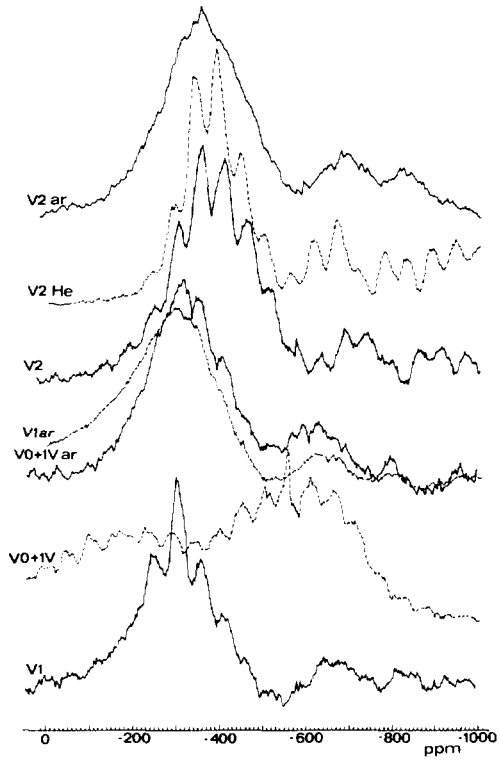

FIG. 2. ^{51}V-MAS-NMR solid-state spectra at room temperature of some selected vanadophosphomolybdic samples. Spinning rate: 4.2 kHz. Chemical shifts are referred to an external standard of $VOCl_3$. For symbols, see text.

and weaker peaks at -542 and -549 ppm. The ^{51}V-NMR spectrum of V2 is characterized by three lines at -532, -539 and -549 ppm (Fig. 3, spectrum 5), in agreement with the literature (*11*, *16*). The presence of multiple lines in the spectrum of V2 apparently suggests the presence of a mixture containing oxoanions with different degrees of substitution of V, according to that suggested for analogous $[PMo_{12-x}W_xO_{40}]^{n-}$ samples (*18*). However, the extensive NMR characterization data of Pope and co-workers (*11*, *16*, *19–22*), Massart *et al.* (*23*), and Domaille (*24*) on heteropolytungstates and molybdates containing vanadium clearly indicate that these multiple peaks must be attributed to different stereoisomers of the $[PMo_{10}V_2O_{40}]^{5-}$ oxoanion and not to oxoanions with a different degree of substitution of vanadium. For the $[PMo_{11}VO_{40}]^{4-}$ oxoanion, on the contrary, different stereoisomers for V are not possible and thus a single ^{51}V-NMR signal must be observed when only this oxoanion is present. The ^{51}V-NMR spectrum in solution of V0 + 1V (Fig. 3) can therefore suggest the presence of the $[PMo_{11}VO_{40}]^{4-}$ and $[PMo_{10}V_2O_{40}]^{5-}$ oxoanions. However, the ^{51}V-MAS-NMR spectrum of the same compound (Fig. 2) does not indicate the presence of these species characterized by a sideband envelope centred around $-300/-400$ ppm, but rather tentatively indicates the presence of $[VO_3]^-$ or $[VO_4]^{3-}$ species (or their oligomers), the ^{51}V-NMR spectrum of which is characterized by a broad absorption around -570 ppm (*14*, *16*, *25*), or $[VO_2(OH_2)_4]^+$ species characterized by a very broad absorption centred around $-540/-580$ ppm (the position depending considerably on the counterion) (*16*). Possibly, when V0 + 1V is dissolved in water, these vanadium species in the secondary structure rapidly exchange

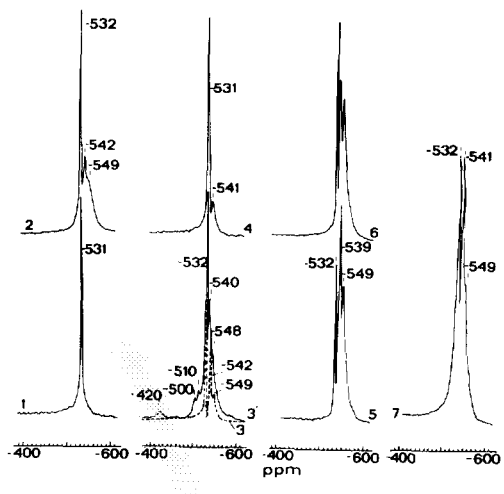

FIG. 3. ^{51}V-NMR spectra in aqueous solution (0.2 *M*) of the same samples as in Fig. 2. Chemical shifts are referred to an external standard of $VOCl_3$. Spectrum (1) V1, (2) V0 + 1V, (3) V1 ar, (3') V1 ar with NH_4VO_3—the molar amount of ammonium vanadate added corresponded to the moles of vanadium in V1, (4) V0 + 1V ar, (5) V2, (6) V2 He, and (7) V2 ar.

with molybdenum ions in the primary structure to form the oxoanion substituted with one or two V atoms. It is known, in fact, that a rapid exchange of structural units between tungsten and molybdenum heteropoly anions is possible (*26*). Apparently, however, this exchange does not occur during the preparation of the V0 + 1V sample. Tentatively, this may be related to the slight reduction of the oxoanion which occurs during the calcination of V0 + *n*V when the organic counter-ion of vanadium (vanadium is added as VO^{2+}-oxalate) is oxidized to CO_2. The slightly reduced oxoanion probably exchanges vanadium rapidly when dissolved in water.

Analysis of the ^{51}V-NMR spectra of V1 and V0 + 1V samples after the catalytic tests (V1 ar and V0 + 1V ar, respectively) gives further indication about this interpretation. The ^{51}V-MAS-NMR spectrum of V1 after the catalytic tests (Fig. 2) shows a main broad and unstructured peak centred at around −300 ppm. The absence of a detectable sideband pattern is reasonably attributed to the broadening of the side-bands induced by the presence of nearby paramagnetic centres (V^{4+} or Mo^{5+}). However, the spectrum overlaps the sideband pattern of the same sample before reaction (Fig. 3, compare spectra V1 and V1 ar), suggesting that after the catalytic tests, the vanadium is still mainly present in the form of the $[PMo_{11}VO_{40}]^{n-}$ oxoanion.

However, the ^{51}V-NMR spectrum in aqueous solution of V1 after the catalytic tests (Fig. 3, spectrum 3–dotted line) shows a main band at −532 ppm just as before reaction (spectrum 1), but also additional weaker bands at −542 and −549 ppm. These additional bands suggest the presence of the oxoanion with two vanadium atoms per Keggin unit. Probably, as indicated before, the oxoanion with two V atoms forms by disproportionation of two oxoanions when the sample (slightly reduced after the catalytic tests) is dissolved in water. It is not possible to exclude altogether that this reaction already occurs in the solid sample and not only when the sample is dissolved, but the analogy of the ^{51}V-MAS-NMR spectra (compare in Fig. 2 the overall lineshape of V1 before and after reaction with that of V2) suggests that the disproportionation occurs in solution.

On the contrary, the solid state ^{51}V-MAS-NMR spectrum of V0 + 1V after the catalytic tests (V0 + 1V ar, Fig. 2) is clearly different from that before reaction and strongly resembles that of the V1 sample. This suggests that in V0 + 1V the exchange reaction between V (in the secondary structure) and Mo (in the primary structure) already occurs in the solid state during the catalytic tests. When dissolved in water (Fig. 3, spectrum 4) this sample gives rise to a main band at −531 ppm as in V1 with a much weaker band at −541 ppm. It is interesting to note that when NH_4VO_3 is added (in a molar amount equivalent to the moles of vanadium in V1) to the solution containing V1 after the catalytic tests (Fig. 3, spectrum 3′) an increase in the bands centred around −540/−550 ppm is observed together with the appearance of new weaker bands at −510, −500, and −420 ppm. The latter three bands can be clearly attributed to the formation of decavanadate ions ($[V_{10}O_{28}]^{6-}$) from ammonium vanadate which, as is known, form in an acid aqueous vanadate solution (in the 3–5 pH range) (*16*). It is also known that in the same solution at lower pH, the $[VO_2]^+$ ion, characterized by a broad ^{51}V-NMR band centred near −545 ppm (*16*), forms. Tentatively, the increase in the −540/−550 ppm region upon addition of ammonium vanadate to the V1 sample after the catalytic tests (compare spectra 3 and 3′ in Fig. 3) can thus be attributed to this vanadayl cation. Possibly, this species is also present in V0 + 1V before and after catalytic reaction.

In the ^{51}V-NMR spectrum in solution of the V2 sample (Fig. 3, spectrum 5) three lines at −532, −539, and −549 ppm are observed, according to literature data (*16, 27*), and these, as discussed above, can be attributed to different stereoisomers of the

$[PMo_{10}V_2O_{40}]^{5-}$ oxoanion. The solid-state ^{51}V-MAS-NMR spectrum of this compound (Fig. 2) shows a resolved set of side bands with the central transition in agreement with the isotropic chemical shift. Tests with different spinning rates suggest that the sideband pattern derives from the overlapping of three distinct sets of sidebands corresponding to the various stereoisomers observed in the spectrum in solution, but the bands are not clearly resolved. The maximum in the peak shape determined by the envelope of side-bands is shifted by about 100 ppm in comparison with the V1 sample.

When V2 is treated in a helium flow at 300°C (30 min) and then cooled to room temperature and exposed to air for some days (V2 He), the ^{51}V-MAS-NMR spectrum remains nearly unchanged (Fig. 2), apart from some additional side-bands centred at around -650 ppm. In the static wide-line ^{51}V-NMR spectrum of vanadophosphomolybdic acids upon a similar treatment, the growth of a strong band is observed centred at -720 ppm and attributed to lacunar or fourfold coordinated vanadium species created during the slightly reducing helium treatment at about 300°C (*6, 15*). This species disappears after forced rehydration at room temperature in air saturated with water vapour (*15*). In our case the additional bands centred around -650 ppm in the V2 He sample (Fig. 2) may be tentatively attributed to the same species. When this sample is dissolved in water (Fig. 3, spectrum 6) the same bands as before the treatment with helium are observed, but with a change in their relative intensities. In particular, there is a considerable increase in the intensity of the band at -532 ppm analogous to that present in the V1 sample.

Also in V2 after the catalytic tests (Fig. 3, spectrum 7) the same three bands are present, but with modified intensity and with an increase in the relative intensity of the -532 ppm component. In the solid-state MAS spectrum of this sample (Fig. 3, V2 ar), due to the broadening induced by the presence of paramagnetic centers (V^{4+} or Mo^{5+}), the sideband pattern is not resolved, but apparently a component centred around -300 ppm increases, suggesting the possible presence of small amounts of the $[PMo_{11}VO_{40}]^{n-}$ oxoanion in this compound.

^{31}P-NMR data. In order to confirm the ^{51}V-NMR results, ^{31}P-NMR spectra were recorded. Table 2 summarizes the main results which are in agreement with the literature data (*11, 16, 23*). In particular, they indicate (i) a progressive downfield shift of the ^{31}P resonance with increasing degree of substitution of Mo with V in the oxoanion due to

TABLE 2

^{31}P-NMR Chemical Shifts (±0.5) of Various Vanadophosphomolybdic Samples

Compound	Treatment	Chemical shift (ppm)		
V0	Calcination	−4.00		
V0 + 1V	Calcination	−3.79(1)	−4.10(0.3)	
V1	Calcination	−3.65		
V2	Calcination	−3.12(1)	−2.42(0.2)	−3.88(0.1)
V0	After catalytic tests	−3.96		
V0 + 1V	After catalytic tests	−3.68(1)	−4.05(0.1)	
V1	After catalytic tests	−3.62(1)	−3.10(0.2)	−3.98(0.1)
V2	After catalytic tests	−3.18(1)	−3.83(0.4)	−2.46(0.3)

Note. Solutions were 0.2 *M* in D_2O; spectra were taken at room temperature, and chemical shifts given are upfield from the external standard (85% H_3PO_4). When multiple peaks are present, the relative intensity with respect to the most intense peak is reported in parentheses.

an increase in the P–O π bonding, (ii) the presence of only one species in the V1 sample, and (iii) the presence of multiple resonances in the spectrum of V2 attributed to the various possible stereoisomers in support of the ^{51}V-NMR data. In fact, in the ^{51}V-NMR spectrum a clear distinction between the presence of different isomers or of oxoanions with different degrees of V substitution is not possible due to the coincidence of resonance lines, but in the ^{31}P-NMR spectrum the resonance lines of V1 do not correspond to those observed for V2.

In the V0 + 1V sample (Table 2) a main resonance line falling at an isotropic chemical shift intermediate between those of V0 and V1 and a weaker additional line near to the value of V0 are observed. This may be tentatively interpreted as the presence of $H_3PMo_{12}O_{40}$ and $H_4PMo_{11}VO_{40}$ oxoanions, but perturbed by coordinated vanadium species (external to the oxoanion). After the catalytic reaction, the V0 + 1V sample shows a main line near to the value of V1 and the relative intensity of the band of the oxoanion without vanadium decreases. In the V1 sample after the catalytic tests new weak lines are observed in comparison with the sample before reaction. The isotropic chemical shift of these new lines is in agreement with the possible formation of the oxoanion containing two vanadium atoms suggested by ^{51}V-NMR data. In the V2 sample after the catalytic tests a slight change is also observed in comparison with the sample before reaction. The change is consistent with the ^{51}V-NMR data about the possible partial leak of one vanadium atom from the oxoanion.

UV–visible diffuse reflectance spectra. Figure 4 shows the UV–visible diffuse reflectance spectra of V0, V2, V0 + 1V and V2 + 1V before and after the catalytic tests ((a) and (b), respectively). Before reaction (spectrum 1), V0 shows a main band centred at 32200 cm^{-1}, the lowest charge transfer (LCT) of Mo^{6+}–O in octahedral coordination (*28*). After the catalytic tests, the spectrum remains similar, but the intensity of the diffuse absorption in the 20,000–13,000 cm^{-1} region (spectrum 5) increases due to the partial reduction of the sample. The spectrum of V2 before reaction (spectrum 2) is similar to that of V0, but an additional band is observed centred at about 21,000 cm^{-1} and reasonably connected with the presence of vanadium in the oxoanion. The attribution of this band cannot be made unequivocally, because, as previously observed (*6*), it falls at a lower frequency than expected for the LCT of octahedral V^{5+} and its relative intensity markedly increases after treatment of the sample in a helium flow at around 300°C. Possible attributions are an intervalence charge transfer (IT) band or LCT of V^{5+} in a strongly distorted environment caused by the dehydroxylation and

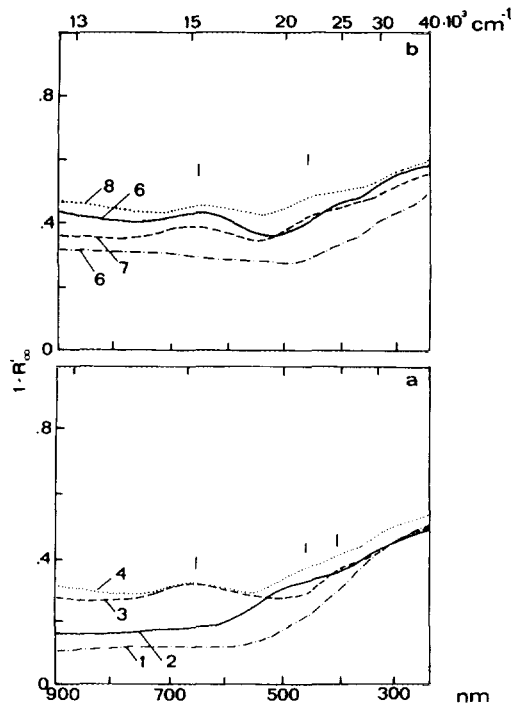

FIG. 4. UV–visible diffuse reflectance spectra of vanadomolybdophosphoric acids (a) before and (b) after the catalytic tests in butadiene oxidation. Spectra before the catalytic tests (after calcination): (1) V0, (2) V2, (3) V0 + 1V, and (4) V2 + 1V. Spectra after the catalytic tests: (5) V0 ar, (6) V2 ar, (7) V0 + 1V ar, and (8) V2 + 1V ar.

partial reduction of the heteropolyanion after the heating treatment (*6*). After the catalytic tests (spectrum 6), a further band is observed centred at about 16,000 cm^{-1} and attributed to the heteronuclear IT $V^{4+} \rightarrow Mo^{6+}$ transition (*29*), because the band occurs at higher frequencies than expected for *d–d* transitions of V^{4+} and shows an enhanced intensity.

In V0 + 1V before the catalytic tests (spectrum 3) two additional bands are observed with respect to V0, centred at about 16,000 and 26,000 cm^{-1}. As discussed above, the first can be attributed to a heteronuclear IT band of V^{4+}. The latter is shifted to higher frequencies with respect to the band at about 21,000 cm^{-1} observed in V2 and can be attributed to the LCT of V^{5+} in a different coordination environment due to its localization outside the oxoanion. After the catalytic tests (spectrum 7), the spectrum strongly resembles that of V2 (spectrum 6). V2 + 1V (spectrum 4) is similar to V0 + 1V and is characterized by an intense band centred at 16,000 cm^{-1} and a not-well-resolved band in the 20,000–30,000 cm^{-1} region, possibly due to the overlapping of the two bands centred at about 21,000 and 26,000 cm^{-1} observed in the V2 and V0 + 1V samples. After the catalytic tests (spectrum 8), the spectrum is analogous to that of V0 + 1V and V2.

Infrared data on the surface acidity. Figure 5 reports spectra of pyridine adsorbed at room temperature on V0 + 1V and V2 samples evacuated at room temperature for 30 min (a) and heated at 160°C for 1 h (b). The V0 + 2V and V2 samples were pretreated in vacuum at 180°C to ensure complete removal of water of crystallization before the adsorption of pyridine. Pyridine adsorption indicates the presence of both Lewis and Brønsted acid sites, characterized by the bands at 1607 cm^{-1} (ν8a), 1487 cm^{-1} (ν19a) and 1446 cm^{-1} (ν19b) for chemisorbed pyridine and by the bands at 1634 cm^{-1} (ν8a,b), 1534 cm^{-1} (ν19b), and 1487 cm^{-1} (ν19a) for the pyridinium ion (*30–32*). Shoulders at 1595 and 1437 cm^{-1} are also found in the spectra recorded after pyridine adsorption on V2, indicating the formation of H-bonded pyridine, but this species disappears after evacuation at room temperature. No great differences are found between V0 + 2V and V2 samples, but in V0 + 2V the band at 1446 cm^{-1} (chemisorbed pyridine) is relatively less intense, whereas the band at 1534 cm^{-1} (pyridinium ion) is relatively more intense. At higher evacuation temperatures, the band at 1446 cm^{-1} disappears in both samples, but more rapidly in the V0 + 2V sample. It should be noted, however, that the band at 1606 cm^{-1} (ν8a) characteristic of Lewis acidity (the extent of the shift of this band with respect to the frequency of 1578 cm^{-1} in the liquid is usually taken as a measure of the strength of the Lewis site (*16, 17*)) does not disappear in parallel with the band at 1446 cm^{-1}.

In order to characterize better the nature of the Lewis acid sites, the adsorption of a weaker base (acetonitrile) was studied. The shift in the stretching frequency of the CN bond with respect to the liquid (2254 cm^{-1}) may be used to evaluate the strength of the Lewis acid sites (*33*). Deuterated acetonitrile was used in order to avoid the presence of a resonance band ($\delta CH_3 + \nu CN$) at around 2300 cm^{-1} (using CH_3CN limits the analysis of the Lewis acid characteristics). Figure 6 reports the spectra obtained for V0, V0 + 2V, and V2 samples after adsorption of CD_3CN at room temperature (1) and evacuation at room temperature (2) or at 100°C (3). The pretreatment of the samples was as for the tests with pyridine (evacuation at 180°C up to complete disappearance of water of crystallization).

For the V0 sample a single band centred at 2307 cm^{-1} is observed. This band is attributed to acetonitrile coordinated on unsaturated Mo^{5+} sites produced by dehydration. The shift with respect to ν_{CN} in liquid acetonitrile indicates the presence of medium-strength Lewis sites (*33*). A shoulder is also observed at around 2260 cm^{-1}, suggesting the possible presence of H-bonded acetoni-

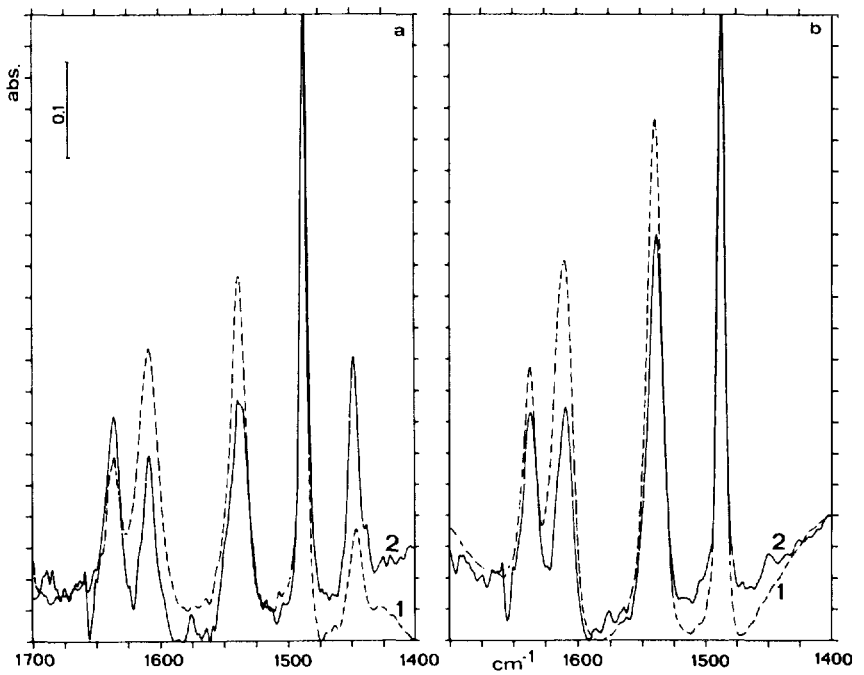

FIG. 5. Infrared spectra of pyridine chemisorption at room temperature (5 Torr) on (1) V0 + 2V and (2) V2 and (a) evacuation at room temperature for 30 min or (b) evacuation at 160°C for 1 h.

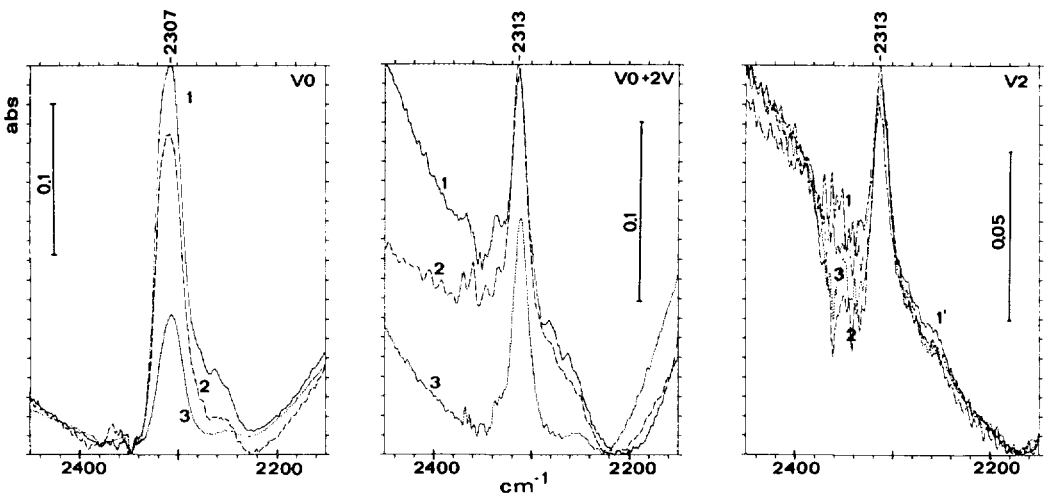

FIG. 6. Infrared spectra of CD_3CN (0.5 Torr) adsorption at room temperature on V0, V0 + 2V, and V2: (1) after adsorption, (2) after evacuation at room temperature for 30 min, and (3) after evacuation at 100°C for 2 h. Also reported for the V2 sample is the spectrum after adsorption at a higher partial pressure (5 Torr) of acetonitrile (1').

trile, but this band disappears upon evacuation. In V0 + 2V the main band shifts to 2313 cm^{-1}, indicating the presence of stronger Lewis acid sites. The intensity of this band decreases after evacuation at 100°C, but the decrease is relatively less intense than in the case of the V0 sample, in agreement with the indication of the presence of stronger Lewis acid sites. These sites are attributed to coordinatively unsaturated VO^{2+} ions, in agreement with the results obtained by acetonitrile adsorption on $(VO)_2P_2O_7$ (*32*). It also should be noted that a single band is present in V0 + 2V, rather than two overlapping bands for molybdenum and vanadium ions. This indicates that when vanadium is present, the reduction occurring during dehydration is localized on the vanadium atom which thus acts to protect molybdenum from reduction. This indication is in agreement with the previous results on the study of the redox properties of molybdovanadophosphoric acids (*6*). Results similar to those of the V0 + 2V sample also are obtained with the V2 sample.

Influence of Vanadium on the Catalytic Behavior

Selective oxidation of butadiene. The catalytic behavior of V0 + nV and V2 + nV as a function of the number of vanadium ions added per oxoanion is summarized in Fig. 7. In order to allow a better comparison of the catalytic behavior of the various samples as indexes of selectivity and activity, the selectivity to maleic anhydride at 95% of butadiene conversion and the reaction temperature for which 95% butadiene conversion is obtained were respectively chosen. All these catalysts completely convert butadiene in the temperature range 240–300°C and the maximum in the selectivity to maleic anhydride is found at the higher conversions (95–100% range of butadiene conversion). The maximum in the selectivity and yield to maleic anhydride (MA) from butadiene is nearly coincident in these catalysts. For example, the catalytic behavior of V0 + 1V and V2 in butadiene oxidation as a function of the reaction temperature is shown in Fig. 8. It should be noted that the order of activity and selectivity determined by the comparison of the catalytic performances at different reaction temperatures (at fixed space-velocity, see Fig. 8) or different space-velocities (at fixed temperature) was not significantly different. Therefore, the differences in the relative activity or selectivity can be related to the reactivity differences of the samples and not to a masking effect of the reaction conditions. Other products of selective oxidation, besides carbon oxides and maleic anhydride, are furan (FU) and crotonaldehyde (CR), which are detected especially at the lower conversions (Fig. 8). Compared in Fig. 9 are the maximum yields in furan and crotonaldehyde from butadiene on V0 + *n*V and V2 + *n*V samples as a function of the number of added V atoms. The temperatures at which the yield in furan is a maximum are also reported.

In V0 + *n*V, the addition of one vanadium atom per oxoanion increases the selectivity to MA with a parallel increase in the specific activity. However, the further addition of a vanadium ion (per oxoanion) drastically decreases both the activity and the selectivity to maleic anhydride with a parallel increase in the formation of carbon oxides. On the contrary, the catalytic behavior of the V2 + *n*V series (Fig. 7) differs from that of the V0 + *n*V series; the addition of vanadium decreases both the activity and the selectivity.

The comparison of V0, V0 + 2V, and V2 samples indicates that better selectivity and activity can be obtained when V ions are present inside the primary structure (oxoanion). However, the comparison of V2 and V0 + 1V samples (Figs. 7 and 8) indicates that similar selectivities and yield in maleic anhydride from butadiene, but different activities, can be obtained either with a catalyst with vanadium inside the oxoanion or with a catalyst prepared by the simple addition of a vanadium component to $H_3PMo_{12}O_{40}$ acid. The latter catalyst is more

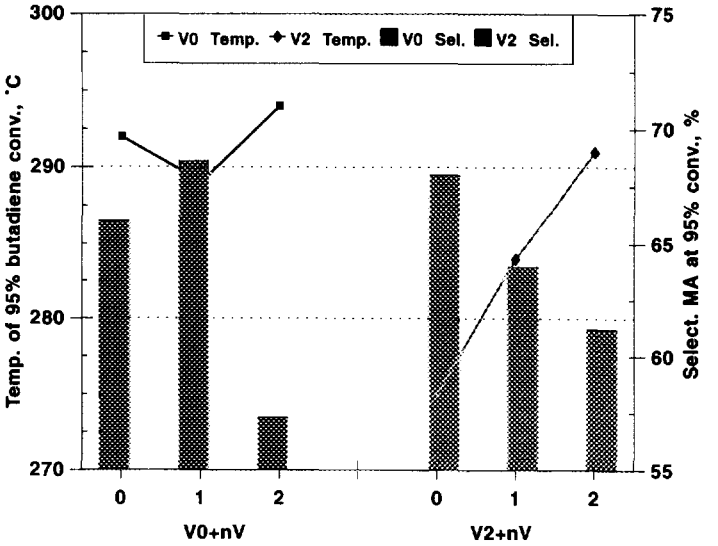

FIG. 7. Comparison of the catalytic behavior of V0 + nV and V2 + nV in butadiene oxidation: temperature of 95% butadiene conversion and selectivity to maleic anhydride (MA) at 95% of butadiene conversion.

selective than an analogous sample, which contains one vanadium ion per oxoanion (V1). The behaviour of the latter in butadiene oxidation, in fact, is in between that shown by V0 and V2, both as regards the activity and the selectivity; therefore, it was not considered necessary also to report the activity of V1. In both V2 and V0 + 1V, the yield of MA decreases considerably for reaction temperatures higher than that of about 98% of conversion, but the decrease is more drastic in V2 (Fig. 8).

The formation of by-products or intermediates of reaction (furan and crotonalde-

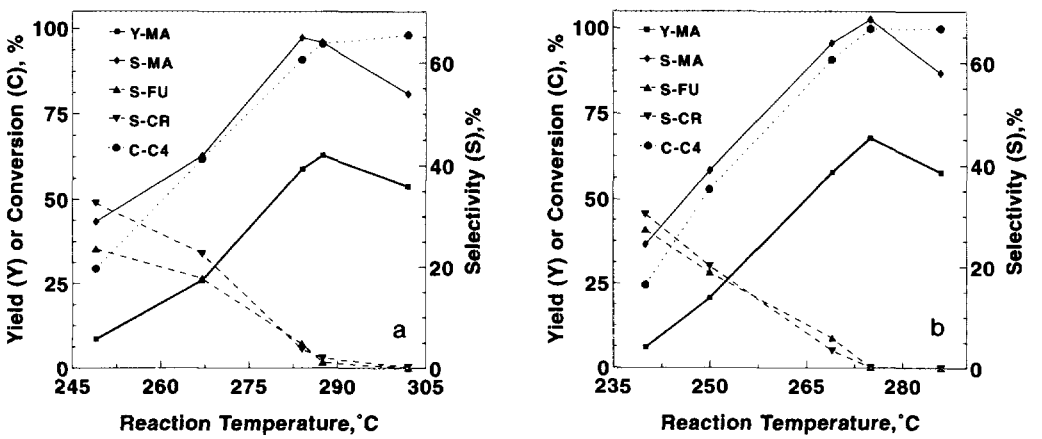

FIG. 8. Catalytic behavior of (a) V0 + 1V and (b) V2 in butadiene oxidation as a function of the reaction temperature. MA, maleic anhydride; FU, furan; CR, crotonaldehyde; C4, butadiene; C, conversion; Y, yield; S, selectivity.

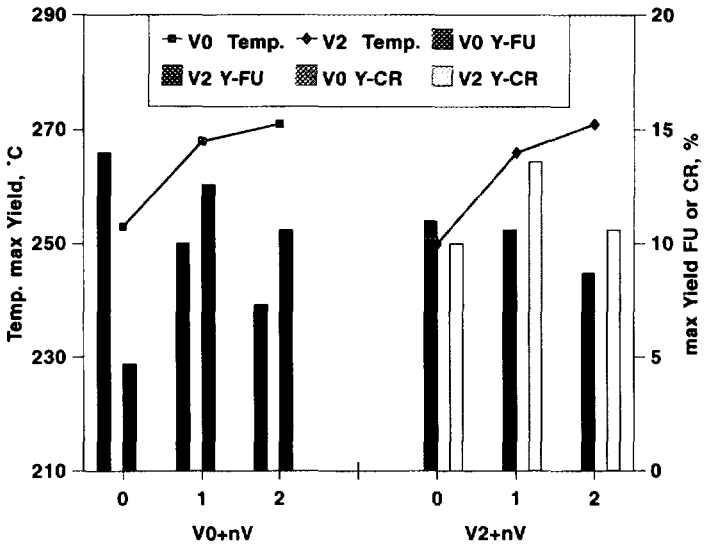

FIG. 9. Comparison of the maximum yield in the formation of by-products (furan and crotonaldehyde) and relative reaction temperature for maximum yield in furan in butadiene oxidation on V0 + *n*V and V2 + *n*V. Symbols as in Fig. 8.

hyde) is slightly affected by the presence of vanadium (Fig. 9). It may be observed that increasing the number of V atoms added per oxoanion increases the temperature of the maximum in the formation of by-products, decreases the maximum yield of furan, and increases that of crotonaldehyde. The differences, however, are limited.

Oxidation of n-butane. The oxidation of *n*-butane occurs over a wider range of temperatures (300–350°C) as compared to butadiene and also lower selectivities to maleic anhydride are found. Furthermore, the selectivity to maleic anhydride passes through a maximum, generally for relatively low conversions of *n*-butane (around 40–50% of conversion). A further increase in butane conversion leads to a considerable increase in carbon oxide formation. In addition, generally a relatively high formation of acetic acid (selectivities around 10%) is observed.

Figure 10 summarizes the catalytic behaviour in *n*-butane oxidation of V0 + *n*V and V2 + *n*V samples. The temperature of 50% conversion of *n*-butane is reported as an index of activity. In the various samples the selectivity to maleic anhydride passes through a maximum with increasing reaction temperature (Fig. 11), but the conversion at which the maximum is reached depends on the sample. For this reason, both the maximum selectivity and yield to maleic anhydride are reported in Fig. 10 as indexes of the selectivity.

In all samples the addition of vanadium ions leads to an increase in the rate of alkane oxidation (Fig. 10), in contrast to the effect shown in butadiene oxidation. The increase in the rate of alkane conversion as a function of the number of added V ions is greater for V0 heteropoly acid than for V2. It can be noted also that V0 + 2V is more active than V2 (Fig. 10), even though the amount of vanadium is the same in the two samples. The opposite trend was observed, on the contrary, in butadiene oxidation (compare V2 and V0 + 2V in Fig. 7).

The presence of vanadium also affects the selectivity to maleic anhydride from *n*-butane and the effect depends both on the amount and localization of vanadium ions. In V0 + *n*V, the addition of V ions leads to an increase in both the maximum selectivity and yield to maleic anhydride. A different

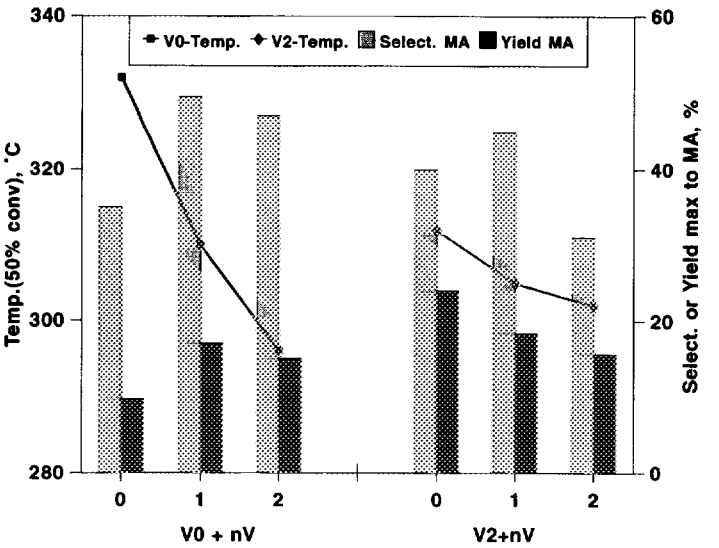

FIG. 10. Comparison of the catalytic behavior of V0 + nV and V2 + nV in n-butane oxidation: temperature of 50% conversion of butane and maximum selectivity and yield to maleic anhydride (MA).

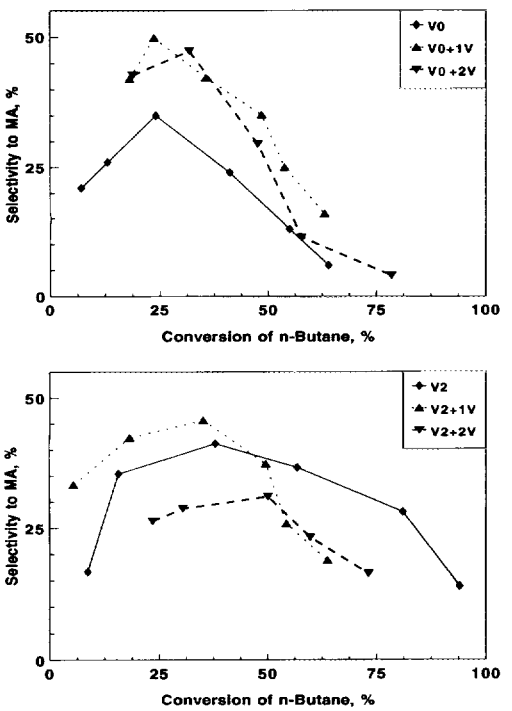

FIG. 11. Dependence of the selectivity to maleic anhydride on the conversion of n-butane (variable reaction temperature) for V0 + nV and V2 + nV.

effect, on the contrary, is observed when vanadium ions are added to V2 (Fig. 10): the maximum yield to MA decreases, but the maximum selectivity to MA initially increases. The addition of V ions to $H_3PMo_{12}O_{40}$ (V0) leads to a considerable increase in the selectivity at low butane conversion (20–40% range) (Fig. 11). For conversions higher than about 50%, the selectivity decreases considerably due to the enhanced rate of consecutive oxidation to carbon oxides. Comparison of the V0 + 2V sample with the V2 sample indicates that, in the first case, V is more selective at low conversion and, in agreement, the addition of one V ion to V2 enhances the selectivity at low conversion (Fig. 11). However, this sample was less selective for conversions higher than about 50%. Better maximum yields to maleic anhydride from butane are thus possible with V2 more than with the other catalyst investigated.

DISCUSSION

The vanadophosphomolybdic heteropoly acid samples patented for gas-phase oxidation reactions contain, in several cases, an

amount of vanadium not exactly equivalent to the stoichiometric value necessary for the insertion of one or two vanadium atoms per oxoanion, but rather an intermediate value. This can be interpreted as optimum behavior when a mixture of oxoanions with a different degree of substitution is present or when some vanadium ions in the secondary structure contribute to the catalytic performances. In addition, some patented procedures for the preparation of these catalysts (for example, by refluxing for 2–3 days an aqueous solution containing a mixture of H_3PO_4, MoO_3, and V_2O_5) are not likely to lead to highly pure samples and the possible presence of vanadium ions in the secondary structure can also be hypothesized.

Therefore, the objective of the study reported in this paper was to determine the role of the localization of vanadium on the catalytic activity of molybdovanadophosphoric acids and to study possible synergic effects when vanadium ions are present both in the primary and secondary structure. On the other hand, a parallel problem was the analysis of the possible changes in the localization of vanadium during the course of the catalytic reaction. Neither of these problems has been thoroughly addressed in the literature. Present data show that complex phenomena occur and therefore that a simple correlation of the catalytic behaviour with the localization of vanadium is not possible, also because changes in the localization during the catalytic reaction occur. More detailed studies will therefore be necessary to clarify these questions further.

Nature and Localization of Vanadium Species in the Fresh Samples

For fresh V1 sample both ^{31}P-NMR (Table 2) and ^{51}V-NMR (Figs. 2 and 3) data agree in indicating the presence of a single oxoanion species containing one vanadium atom. Infrared data (Fig. 1 and Table 1) also are in agreement with this indication. All characterizations, therefore, indicate the presence of a nearly pure $H_4PVMo_{11}O_{40}$ compound in the calcined sample. In fresh V2, the presence of a nearly pure $H_5PV_2Mo_{10}O_{40}$ compound is more questionable, because both ^{31}P-NMR (Table 2) and ^{51}V-NMR (Figs. 2 and 3) data indicate the presence of multiple signals. This result is in good agreement with the literature data for phosphovanadomolybdo- and phosphovanadotungstooxoanions containing two vanadium atoms (*16, 20, 21, 24, 27, 34*). All these authors related the presence of multiple signals to the presence of different geometric isomers, in contrast to other authors (*18*), who interpret the multiple signal in the ^{31}P-NMR spectrum as indicative of the presence of oxoanions with a different degree of substitution. Our results are in accordance with the first well-documented interpretation. In particular, ^{31}P-NMR data (Table 2) clearly indicate that the presence of $[PMo_{12}O_{40}]^{3-}$ and $[PVMo_{11}O_{40}]^{4-}$ oxoanions in the V2 sample may be reasonably excluded; if present they must be in very low, undetectable amounts. Infrared data (Fig. 1 and Table 1) are in agreement with this conclusion.

In V0 + 1V, ^{31}P-NMR (Table 2), and ^{51}V-NMR (Fig. 3) spectra in the liquid phase suggest the presence of the oxoanion containing one V atom, even though perturbed by the presence of vanadium external to the oxoanion. However, ^{51}V-MAS-NMR data in the solid phase (Fig. 2) exclude the presence of this compound in V0 + 1V before the catalytic tests, unless in very low amounts. Infrared data on the solid sample (Fig. 1) confirm this indication. In particular, the shift of the P–O and Mo–O stretching frequencies (Table 1) and the shoulder at 1085 cm^{-1} due to the lowering of the symmetry of the oxoanion when vanadium is present inside the oxoanion are absent. This suggests that the exchange in position of vanadium and molybdenum to form the oxoanion containing one vanadium atom occurs mainly when the sample is dissolved in water. As discussed before, this may be connected to the slight reduction of the sample induced during calcination by combustion of the organic material introduced during the addition of the vanadium component.

UV–visible diffuse reflectance spectra of V0 + 1V before reaction (Fig. 4) show the presence of both V^{4+} and V^{5+} ions. The former are shown by the presence of an intense band near 16,000 cm^{-1} attributed to heteronuclear intervalence $V^{4+} \rightarrow Mo^{6+}$ charge transfer. This shows also that the V^{4+} ion and the Mo^{6+} ions of the oxoanion must be in close proximity. ^{31}P-NMR data (Table 2), on the other hand, indicate a perturbation of the oxoanion, possibly connected with the effect of the external vanadyl ions interacting with the Keggin anion. The UV–visible diffuse reflectance spectrum of V0 + 1V also shows the presence of V^{5+} ions characterized by an absorption centred near 26,000 cm^{-1} which is shifted by about 5000 cm^{-1} with respect to that observed in the samples containing one or two vanadium atoms per Keggin anion. The band is attributed to the LCT of $[VO_2]^+$ ions in a nearly octahedral coordination. The ^{51}V-MAS-NMR spectrum (Fig. 2), even though very weak, is in agreement with the presence of a $[VO_2{-}(OH_2)_4]^+$ species. This V^{5+} species after dissolution in water, apart from that reacting with the oxoanion, is evidenced in the ^{51}V-NMR spectrum (Fig. 3) by a broad band centred near −545 ppm. This band is attributed to $[VO_2]^+$ ions on the basis of the tests with added ammonium vanadate. It should be pointed out that when ammonium vanadate is added to the NMR solution, the formation of the decavanadate ion can also be clearly shown. The absence of its ^{51}V-NMR bands in the spectrum of V0 + 1V in solution suggests the probable absence of the decavanadate ion in the V0 + 1V sample. Infrared data (Fig. 1) confirm the absence of this compound and also clearly exclude the presence of V_2O_5. The frequency of the band observed (around 990 cm^{-1}) corresponds to that shown by well dispersed and hydrated V^{5+} in nearly octahedral coordination on TiO_2 (*35*). In addition, this V^{5+} species also shows a UV–visible diffuse reflectance band centred near 26,000 cm^{-1} (*36*).

Finally, it should be mentioned that no significant difference in the surface area of the samples containing vanadium in the oxoanion or prepared by simple addition of V oxalate to V0 and V2 heteropoly acids was found. In all cases the surface area ranges from 4 to 8 m^2/g and there is no significant increase in the surface area as observed, for example, when these heteropoly acids are salified with alkali metals (*11*). Similar observations have been made when $H_4PVMo_{11}O_{40}$ was salified with La^{3+} (*37*). On the other hand, infrared data on the surface acidity of these samples (Fig. 5) indicate the presence of Brønsted acid sites when vanadium is in both the secondary or primary structure.

In conclusion, the characterization of the fresh phosphovanadomolybdo samples indicates that in the starting samples for the catalytic tests the presence of vanadium only in the primary or secondary structure may be reasonably assumed. In the former case, vanadium is present as V^{5+} in nearly octahedral coordination substituting for one or more molybdenum atoms of the $[PMo_{12}O_{40}]^{3-}$ oxoanion. In the latter case, vanadium is tentatively assumed to be present as mixed valence VO^{2+}–VO_2^+ hydrated complexes localized in the secondary structure, but interacting with the oxoanion.

Changes Occurring during the Catalytic Reaction

UV–visible diffuse reflectance spectra (Fig. 4) of the samples after the catalytic tests indicate that in all samples a partial reduction of the vanadium occurs during the reaction, in agreement with previous indications (*6*). However, NMR data suggest also the possibility of a partial change in the localization of vanadium. This is clearly evident in the case of V0 + 1V, where the ^{51}V-MAS-NMR spectrum (Fig. 2) shows the partial formation of the oxoanion containing one vanadium atom after the catalytic tests. The presence of water vapour (product of reaction) in combination with the reducing action of the hydrocarbon presumably enhances the rate of exchange between molyb-

denum atoms of the oxoanion and the external vanadium ions. This also shows the easy migration and exchange which can occur during the catalytic oxidation of hydrocarbons.

In agreement with this indication, NMR data on the samples containing vanadium only in the primary structure (V1 and V2) show that a partial transformation occurs after the catalytic reaction. The data do not allow an unequivocal conclusion about this aspect, but tentatively suggest the possible partial leakage of vanadium from the oxoanion and creation of partial lacunar situations. On the other hand, the catalytic activity of these samples is comparable with that of previous results (*6*, *7*) and was relatively stable in a laboratory time-scale (some days). When decomposition of the oxoanion occurs for reaction temperatures higher than about 360°C, these samples become completely inactive and therefore their catalytic activity or changes with time-on-stream can monitor the occurrence of possible reactions of irreversible decomposition of the Keggin oxoanion. The nature of the thermal transformations at temperatures of 300–350°C or during the catalytic tests has already been discussed in detail for similar samples (*6*, *7*). It should be mentioned, in particular, that scanning electron microscopy data (*7*) indicate the partial surface amorphization of the sample (creation of large regions with a smooth surface), but without irreversible destruction of the oxoanion structure. Recently, results of an investigation using $Cr[PMo_{12}O_{40}]$ samples (*38*) also suggested the possibility of formation of an amorphous material which lost its long-range order, but preserved the local Keggin-anion structure. It was suggested (*38*) that the presence of Cr^{3+} in the secondary structure alters the temperature stability range of this pseudoamorphous phase in comparison to phosphovanadomolybdic acids and they proposed a role for this amorphous phase in the catalytic activity of these samples. The present results do not allow further clarification of this point, but our data on the nature of the possible changes after the catalytic tests are in agreement with the formation of this pseudo-amorphous phase which can explain the above mentioned effect. In addition, infrared data (Figs. 5 and 6) show the presence of Lewis sites with similar acid strength in both V0 + 2V and V2. The infrared evacuation treatment used in this study was a complete dehydroxylation which probably induces very similar effects (especially in terms of reduction) as those observed after the catalytic tests. We have previously shown (*6*) that the complete dehydroxylation can be monitored by following the changes in the overtone region of the skeletal vibrations (around 2000–2100 cm^{-1}). After complete dehydroxylation, a change in these overtone bands is observed in comparison with the situation after complete removal of water of crystallization. However, the initial situation can be reversibly recreated by adding water vapour. On the contrary, for higher temperatures of evacuation, an irreversible destruction of the Keggin anion occurs. The observation of Lewis acid sites refers to the case of reversible transformation, before the irreversible destruction. In previous studies on the surface acidity the pretreatment probably only removed water of crystallization, without complete dehydroxylation, and this can explain why the presence of Lewis acid sites was not observed (*4*, *9*). However, probably the type of evacuation procedure used in our tests is more representative of the types of transformation occurring during the catalytic reaction, especially in alkane oxidation. Significantly, infrared data show the same type of Lewis acid sites in both V0 + 2V and V2 samples and this can be better understood on the basis of the previously discussed hypothesis of reversible amorphization in dehydroxylated samples.

Finally, it should be mentioned that the presence of vanadium ions in the secondary structure can alter the mechanism of formation of this phase. We have, in fact, observed (*39*) significant differences in the thermal behaviour in a thermobalance when

vanadium is localized in the primary and secondary structure, but further studies in order to analyze these effects better are necessary. The investigation of the influence of the presence of La^{3+} ions in the secondary structure of phosphovanadomolybdic acids (*37*) has also shown the influence of the presence of transition metals on the mechanism of thermal transformation and dehydroxylation. Strong analogies with the effect of Cr^{3+} (*38*) can be noted. Possibly, also vanadium ions in the secondary structure can have similar effects, but the possibility of exchange with the molybdenum atoms of the oxoanion shown in the case of V0 + 1V makes any clear conclusion about this aspect more difficult.

Relationship between Catalytic Behavior and Localization of Vanadium

The comparison of the effect of the addition of vanadium to V0 and V2 illustrates a basic difference between the oxidation of butadiene (Fig. 7) and of *n*-butane (Fig. 10). In the first case the addition of vanadium deactivates the catalyst, whereas in the latter case it promotes the activity. We have already observed (*7*) a linear correlation between the rate of alkane (n-pentane) oxidation and the number of vanadium atoms in $H_{3+n}PV_nMo_{12-n}O_{40}$ (n = 0–2) samples. The comparison of the activity of V0 and V2 in butadiene and *n*-butane oxidation confirms this indication, in agreement with the literature (*5*). Vanadium has enhanced catalytic properties with respect to molybdenum (*3*) and therefore it is reasonable to observe a correlation between the amount of vanadium in the catalyst and the rate of hydrocarbon oxidation. Due to the effect of surface Lewis activity of activated samples (Fig. 6) one may also speculate a relationship between the formation of stronger Lewis acid sites and the rate of hydrocarbon activation, by analogy with the evidence on this relationship observed for *n*-butane oxidation to maleic anhydride on vanadium–phosphorus oxides (*40*). In agreement, in *n*-butane oxidation on phosphovanadomolybdic acids (Fig. 10), the activity of the catalyst is proportional to the amount of vanadium and increases proportionally with the amount of vanadium added for both V0 + nV and V2 + nV samples. Apparently, the increase in the rate of alkane conversion as a function of the number of V ions added is more drastic for the V0 + nV series than for the V2 + nV series. It can be noted also that V0 + 2V is more active than V2 (Fig. 10). Possibly, the localization of vanadium ions influences their turnover frequency, but the differences are not very relevant when taking into account the changes discussed before in the localization during the course of the catalytic reaction. A clear conclusion about the relationship between localization of vanadium and rate of *n*-butane oxidation thus cannot be derived, but the good agreement between the various results indicates a correlation between amount of vanadium and activity when the vanadium atoms are localized before reaction in the primary or secondary reaction.

Surprisingly, on the contrary, the addition of vanadium inhibits the conversion of butadiene (Fig. 7). This is clearly evident for the V2 + nV series, whereas for the V0 + nV series apparently the activity passes through a maximum, even though the differences are minor. On the other hand, V0 is less active than V2 and therefore the addition of vanadium to V0 initially improves the activity, whereas for higher vanadium contents the inhibition effect prevails (see V2 + nV series). An explanation of the different effects of the addition of vanadium in the case of *n*-butane and butadiene can reasonably be based on the difference in their rate limiting step of catalytic transformation. According to an analogy with vanadium–phosphorus oxides ((*40*) and references therein) in butadiene oxidation the rate determining step is the insertion of oxygen into the adsorbed butadiene, whereas in *n*-butane the H-abstraction step to activate the alkane is rate determining. On chromium 12-molybdophosphate catalysts with the Cr^{3+} in cationic positions (*38*), it was suggested that in

the temperature range of formation of the pseudo-amorphous phase discussed above (380–480°C) the catalyst is selective in oxidative dehydrogenation of propane to propylene which is not further oxidized to acrolein, whereas at lower temperatures this sample is an efficient catalyst for nucleophilic addition of oxygen (pentane to maleic anhydride). The authors hypothesized that the formation of the pseudo-amorphous phase (reversible transformation of the Keggin anion with loss of the long-range order, but preserving short-range order of the oxoanion) is responsible for this difference in the catalytic properties.

More investigation will be necessary to clarify the deactivation effect in butadiene oxidation when a vanadium component is added in the secondary structure, but tentatively it can be proposed that the effect is connected with changes in the mechanism of dehydration and reversible transformation of the Keggin anion induced by the presence of transition metal ions in the secondary structure. This effect clearly remains also when vanadium exchanges with molybdenum atoms of the oxoanion.

The addition of vanadium also has a considerable influence on the selectivity. In butadiene oxidation (Fig. 7), the trend follows that of activity. For V2, the addition of vanadium causes a parallel decrease in the selectivity and the activity. For V0 the selectivity passes through a maximum in correspondence with the minimum in activity. The parallelism is reasonable taking into account that, as mentioned above, the rate limiting step is the insertion of oxygen into the adsorbed butadiene.

In *n*-butane oxidation, on the contrary, no direct relationship is observed between the activity and selectivity with the addition of vanadium (Fig. 10). This agrees with the different rate limiting steps. In V0 + *n*V, the addition of V ions in the secondary structure leads to an increase in both the maximum selectivity and yield to maleic anhydride. A different effect, on the other hand, is observed when vanadium ions are introduced into the secondary structure of V2 (Fig. 10): the maximum yield to MA decreases, but the maximum selectivity to MA initially increases. The analysis of the dependence of the selectivity to maleic anhydride on the conversion of *n*-butane (Fig. 11) suggests that V ions inside the oxoanion and in the secondary structure have different effects on the synthesis of maleic anhydride from *n*-butane. The addition of V in the secondary structure of V0 (before the catalytic tests) leads to a considerable increase in the selectivity at low butane conversion (20–40% range). For conversions higher than about 50%, the selectivity decreases considerably due to the enhanced rate of consecutive oxidation to carbon oxides. The comparison of the V0 + 2V sample with the V2 sample indicates that V in the secondary structure (before the catalytic tests) is more selective at low conversion and, in agreement, the introduction of one V ion in the secondary structure of V2 enhances the selectivity at low conversion (Fig. 11). However, this sample was less selective for conversions higher than about 50%. Better maximum yields to maleic anhydride from butane are thus possible with V2 more than with the other catalysts investigated.

REFERENCES

1. Tsigdinos, G. A., *Top. Curr. Chem.* **76,** 1 (1978).
2. (a) Misono, M., *Catal. Rev.-Sci. Eng.* **29,** 269 (1987); (b) Misono, M., *Catal. Lett.* **12,** 63 (1992).
3. Ono, Y., *in* "Perspectives in Catalysis" (J. M. Thomas and K. I. Zamaraev, Eds.), p. 431. Blackwell, Oxford, 1992.
4. (a) Brückman, K., Haber, J., and Serwicka, E. M., *Faraday Discuss. Chem. Soc.* **87,** 173 (1989); (b) Serwicka, E. M., Brocławik, E., Brückman, K., and Haber, J., *Catal. Lett.* **2,** 351 (1989).
5. (a) Ai, M. *in* "Proceedings, 8th International Congress on Catalysis, Berlin, 1984," Vol. 5, p. 475. Verlag Chemie, Weinheim, 1964; (b) Ai, M., *J. Catal.* **85,** 324 (1984).
6. Centi, G., Lena, V., Trifirò, F., Ghoussoub, D., Aïssi, C. T., Guelton, M., and Bonnelle, J. P., *J. Chem. Soc. Faraday Trans.* **86,** 2775 (1990).
7. Centi, G., Lopez Nieto, J., Iapalucci, C., Brückman, K., and Serwicka, E. V., *Appl. Catal.* **46,** 197 (1989).
8. (a) Jerschkewitz, H.-G., Alsdorf, E., Fichtner, H., Hanke, W., Jancke, K., and Öhlmann, G. Z.,

Anorg. Allg. Chem. **526,** 73 and 86 (1985); (b) Jerschkewitz, H.-G., Alsdorf, E., and Öhlmann, G., *J. Chem. Soc. Faraday Trans. I* **82,** 3479 and 3491 (1986).
9. Bielanski, A., Malenka, A., and Kubelkova, L., *J. Chem. Soc. Faraday Trans. I* **85,** 2847 (1989).
10. Kutyrev, M. Yu., Staroverova, I. N., Thiep, N. Z., and Krylov, O. V., *in* "New Developments in Selective Oxidation" (G. Centi and F. Trifirò, Eds.), p. 869. Elsevier, Amsterdam, 1990.
11. Pope, M. T., *in* "Comprehensive Coordination Chemistry" (G. Wilkinson, R. D. Gillard, and J. A. McCleverty, Eds.), Vol. 3, p. 1023. Pergamon, Oxford, 1989.
12. Tsigdinos, G. A., and Hallada, C. J., *Inorg. Chem.* **7,** 137 (1968).
13. Rocchiccioli-Deltcheff, C., Thouvenot, R. R., and Frank, R., *Spectrochim. Acta Part A* **32,** 587 (1976).
14. Eckert, H., and Wachs, I. E., *J. Phys. Chem.* **93,** 6796 (1989).
15. Taouk, B., Ghoussoub, D., Bennani, A., Crusson, E., Rogole, M., Aboukais, A., Decressain, R., Fournier, M., and Guelton, M., *J. Chim. Phys.-Chim. Biol.* **89,** 435 (1992).
16. O'Donnel, S. E., and Pope, M. T., *J. Chem. Soc. Dalton Trans.*, 2290 (1976).
17. Lapina, O. B., Simakov, A. V., Mastikhin, V.M., Veniaminov, S. A., and Shubin, A. A., *J. Mol. Catal.* **50,** 55 (1989).
18. Black, J. B., Clayden, M. J., Griffiths, I., and Scott, J. D., *J. Chem. Soc. Dalton Trans.*, 2765 (1984).
19. Harmalker, S. P., Leparulo, M. A., and Pope, M. T., *J. Am. Chem. Soc.* **105,** 4286 (1983).
20. Pope, M. T., O'Donnel, S. E., and Prados, R. A., *J. Chem. Soc. Chem. Commun.*, 22 (1975).
21. Leparulo-Loftus, M. A., and Pope, M. T., *Inorg. Chem.* **26,** 2113 (1987).
22. Pope, M. T., and Scully, T. F., *Inorg. Chem.* **14,** 952 (1975).
23. Massart, R., Constant, R., Fruchart, J.-M., Ciabrini, J.-P., and Fournier, M., *Inorg. Chem.* **16,** 2917 (1977).
24. Domaille, P. J., *J. Am. Chem. Soc.* **106,** 7677 (1984).
25. Crans, D. C., Rithner, C. D., and Thisen, L. A., *J. Am. Chem. Soc.* **112,** 2901 (1990).
26. Schwegler, M. A., Peter, J. A., and van Bekkum, H., *J. Mol. Catal.* **63,** 343 (1990).
27. Neumann, R., and Levin, M., *J. Am. Chem. Soc.* **114,** 7278 (1992).
28. So. H., and Pope, M., *Inorg. Chem.* **11,** 1441 (1972).
29. Altenau, J. J., Pope, M., Prados, R. A., and So, H., *Inorg. Chem.* **14,** 417 (1975).
30. Boehm, H.-P., and Knözinger, H., *in* "Catalysis Science and Technology" (J. R. Anderson and M. Boudart, Eds.), Vol. 4, p. 39. Springer-Verlag, Berlin, 1983.
31. Morterra, C., Ghiotti, G., Garrone, E., and Fisicaro, E., *J. Chem. Soc. Faraday Trans. I* **76,** 2102 (1980).
32. Busca, G., Centi, G., Trifirò, F., and Lorenzelli, V., *J. Phys. Chem.* **90,** 1337 (1986).
33. Knözinger, H., and Krietenbrink, H., *J. Chem. Soc. Faraday Trans. I* **71,** 2421 (1975).
34. Kuznetsova, L. I., Maksimovskaya, R. I., Subocheva, O. A., and Matveev, K. I., *Kinet. Katal. (Engl. Transl.)* **27,** 695 (1986).
35. Centi, G., Pinelli, D., Trifirò, F., Ghoussoub, D., Guelton, M., and Gengembre, L., *J. Catal.* **130,** 238 (1991).
36. Busca, G., Centi, G., Marchetti, L., and Trifirò, F., *Langmuir* **2,** 568 (1986).
37. Tonghao, W., Yuchun, L., Hongmao, Y., Guojia, W., Hengbin, Z., Shiying, H., Yuzi, J., and Kaiji, Z., *J. Mol. Catal.* **57,** 193 (1989).
38. Brückman, K., and Haber, J., *in* "Proceedings, 10th International Congress on Catalysis, Budapest, 1992, p. 741. Akadémiai Kiadó/Elsevier, Budapest/Amsterdam, 1993.
39. Lena, V., *Thesis*, Univ. of Bologna, Italy, 1989.
40. Centi, G., Trifirò, F., Ebner, J. R., and Franchetti, V. M., *Chem. Rev.* **88,** 55 (1988).